El Niño–Induced Tropical Droughts in Climate Change Projections

CAIO A. S. COELHO

Centro de Previsão de Tempo e Estudos Climáticos, Instituto Nacional de Pesquisas Espaciais, Cachoeira Paulista, Brazil

LISA GODDARD

International Research Institute for Climate and Society, The Earth Institute at Columbia University, New York, New York

(Manuscript received 6 April 2009, in final form 8 July 2009)

ABSTRACT

El Niño brings widespread drought (i.e., precipitation deficit) to the tropics. Stronger or more frequent El Niño events in the future and/or their intersection with local changes in the mean climate toward a future with reduced precipitation would exacerbate drought risk in highly vulnerable tropical areas. Projected changes in El Niño characteristics and associated teleconnections are investigated between the twentieth and twenty-first centuries. For climate change models that reproduce realistic oceanic variability of the El Niño–Southern Oscillation (ENSO) phenomenon, results suggest no robust changes in the strength or frequency of El Niño events. These models exhibit realistic patterns, magnitude, and spatial extent of El Niño–induced drought patterns in the twentieth century, and the teleconnections are not projected to change in the twenty-first century, although a possible slight reduction in the spatial extent of droughts is indicated over the tropics as a whole. All model groups investigated show similar changes in mean precipitation for the end of the twenty-first century, with increased precipitation projected between 10°S and 10°N, independent of the ability of the models to replicate ENSO variability. These results suggest separability between climate change and ENSO-like climate variability in the tropics. As El Niño–induced precipitation drought patterns are not projected to change, the observed twentieth-century variability is used in combination with model-projected changes in mean precipitation for assessing year-to-year drought risk in the twenty-first century. Results suggest more locally consistent changes in regional drought risk among models with good fidelity in reproducing ENSO variability.

1. Introduction

The majority of drought-related hazards and the attendant economic losses and mortality risks reside in the tropics (Dilley et al. 2005). Changes in climate variability, including more frequent and damaging extreme events such as drought, is one of many anticipated impacts of climate change. Estimating how climate variability may change in a warmer world, and how that variability intersects with more slowly evolving climate change, is vitally important to climate risk management and adaptation efforts.

El Niño plays the largest role in tropical drought occurrence. For a substantial fraction of the tropics, severe droughts in the meteorological sense (i.e., precipitation deficit) develop preferentially during El Niño events (Lyon 2004). Furthermore, the severity and extent of tropical droughts exhibit a fairly linear relationship to the strength of El Niño events (Lyon 2004). The possibility of increases in the strength or frequency of El Niño events in a warmer future climate have clear negative societal implications for many of the already vulnerable tropical land areas.

Numerous uncertainties surround El Niño and climate change in coupled general circulation models (CGCMs). First, although the latest models developed for the 2007 Intergovernmental Panel on Climate Change (IPCC) Fourth Assessment Report (AR4)—the so-called phase 3 of the Coupled Model Intercomparison Project (CMIP3) models—have improved their representation of El Niño–Southern Oscillation (ENSO) characteristics relative to their predecessors (AchutaRao and Sperber 2006), representations of ENSO variability remain imperfect.

Corresponding author address: Caio Coelho, Centro de Previsão de Tempo e Estudos Climáticos, Instituto Nacional de Pesquisas Espaciais, Rodovia Presidente Dutra, KM 40, SP-RJ, 12630-000, Cachoeira Paulista, SP, Brazil.
E-mail: caio.coelho@cptec.inpe.br

DOI: 10.1175/2009JCLI3185.1

Second, it has been suggested that the CMIP3 models disagree on whether El Niño events will become stronger or more frequent, subject to increasing greenhouse gasses (e.g., Meehl et al. 2007, cf. their Fig. 10.16). Looking at patterns of sea level pressure associated with ENSO, van Oldenborgh et al. (2005b) found that the CMIP3 models disagreed on whether the temporal variance of indices associated with those patterns would increase or decrease by the end of the twenty-first century. They stated that in the cases where notable changes did exist they were of the same order as the observed 1866–2004 variance in the Southern Oscillation index (SOI), and thus not significant. Merryfield (2006) examined the variances of principal component time series of the leading empirical orthogonal function (EOF) of tropical Pacific monthly sea surface temperature (SST) anomalies, representative of ENSO, from double carbon dioxide climate simulations compared to preindustrial climate simulations and, based on a *t* test, determined whether the differences between the two simulations lay significantly outside of the range set by several century-long preindustrial cases in each model. Four of the 15 models examined exhibited differences that exceeded the 5% confidence level, but half of those showed increased amplitude in ENSO variability and the other half showed decreased amplitude. However, this measure may incorporate both spatial and temporal changes within the tropical Pacific that could cancel each other. The conclusion from these studies as well as others is that no firm projection about the future behavior of El Niño variability can be made because the models disagree.

Also discussed in the context of climate change is whether the mean state of the tropical Pacific will come to look more El Niño– or La Niña–like. This phrasing of mean state change implicitly suggests that the mean tropical climate will as well move toward conditions realized in those phases of ENSO. Climate change models do not agree on whether the spatial pattern of tropical SST changes will resemble El Niño, although according to some studies there may be a slightly greater likelihood for a more El Niño–like future than La Niña–like future (e.g., Collins et al. 2005). This constitutes a third aspect of uncertainty related to El Niño and climate change. Studies supporting a more La Niña–like future base their arguments primarily on ocean mechanisms, while those suggesting a more El Niño–like future have arguments focused on atmospheric mechanisms. Vecchi et al. (2008) suggest that the particular ENSO-like tendency of a model depends on the relative role of ocean versus atmosphere in the tropical Pacific response to increasing greenhouse gasses. The more La Niña–like response arises from the ''ocean thermostat'' mechanism (Clement et al. 1996) in which eastern equatorial Pacific upwelling reduces ocean surface warming from increased longwave radiative forcing, thus strengthening the zonal temperature gradient between eastern and western Pacific. The more El Niño–like response follows from a weakening of the Pacific Walker circulation as precipitation efficiency increases in a warmer, moister world. Such weakening leads to a reduction in the easterlies in the equatorial Pacific, which results in a reduction in the equatorial Pacific east–west SST gradient. Simplifications in ocean mixed layer dynamics common in the current generation of coupled models is likely to be responsible for the relatively weak role of ocean dynamics and thus a greater tendency toward an El Niño–like mean state in the future (Vecchi et al. 2008).

Much this concern over change in the tropical Pacific mean state and its variability arises from the expected impact those changes will have on the climate. Potentially, similar physical mechanisms lead to tropical drying/drought associated with El Niño events and climate change (Neelin et al. 2003). How will the teleconnections observed during El Niño, and in particular tropical droughts, change in the future? In a relative sense, even if ENSO variability were to remain constant, will changes in the mean state modify the teleconnections? Or, in an absolute sense, how will changes in the tropical Pacific mean state intersect with El Niño teleconnections to modify the risk of drought? Sterl et al. (2007) found little evidence for changes in the strength of ENSO atmospheric teleconnections in the twenty-first century. This study focuses on the precipitation signature of these teleconnections and how they will be realized in the future given the possible changes in the mean state. We investigate the extent to which precipitation changes, particularly the negative changes related to precipitation deficit, interact or intersect with ENSO variability. Studies have examined how ENSO itself may change, and others have looked at regional precipitation changes, but little has been done on how ENSO teleconnections—particularly El Niño–induced drought patterns—together with projected precipitation changes in the tropics can inform the changing risk of drought conditions.

This study first evaluates the patterns, magnitude, and spatial extent of El Niño–induced tropical droughts during a control period in the twentieth century in climate simulations, which have realistic evolution of greenhouse gasses. Next it examines the projected changes in the characteristics of El Niño and in the strength of the identified patterns of El Niño–induced tropical drought in the twenty-first century. Finally, the patterns of mean precipitation changes are examined to assess whether those changes exacerbate or ameliorate the risk of El Niño–induced drought conditions in the twenty-first century. The use of the term drought in this study is

the simple meteorological definition of precipitation deficits. Clearly, as the climate warms, and the atmospheric evaporative demand increases, water availability will decrease even if precipitation totals remain constant (e.g., Wang 2005; Easterling et al. 2007; McCabe and Wolock 2007). Temperature changes in the tropics are likely to be smaller than the global average and will be much more spatially homogenous than mean precipitation changes. Previous studies provided comprehensive analysis of agricultural (Wang 2005) and hydrological (Nohara et al. 2006; Hoerling and Eischeid 2007) droughts in CMIP3 simulations. The investigation performed here complements these previous studies focusing on meteorological droughts in CMIP3 simulations during El Niño events. The interest here is to assess

- projected changes in El Niño magnitude and frequency relative to the twentieth-century characteristics of El Niño variability;
- changes in El Niño–induced tropical teleconnections in the twenty-first century relative to those in the twentieth century; and
- the manner in which El Niño–induced tropical teleconnections intersect with twenty-first-century precipitation change.

The manuscript is structured as follows: Section 2 describes the datasets and approach used in the investigation. Section 3 presents an analysis of model-projected changes in El Niño itself between the twentieth and twenty-first centuries and also examines the ability of the coupled models to simulate tropical teleconnections associated with El Niño variability during the twentieth century. Sections 4 and 5 examine how ENSO-induced drought patterns change in the twenty-first century and how such patterns can be combined with projected mean precipitation changes for estimating El Niño–induced drought risk in the twenty-first century. Section 6 concludes the manuscript with a summary and discussion of the findings.

2. Datasets and investigation approach

El Niño precipitation teleconnections are reasonably well reproduced by seasonal climate models (van Oldenborgh et al. 2005a; Coelho et al. 2006) and therefore provide comparative perspective for CMIP3 simulations. For this reason, this study is performed using the following climate models:

- Three Development of a European Multimodel Ensemble System for Seasonal-to-Interannual Prediction (DEMETER) (Palmer et al. 2004) coupled seasonal forecast models [European Centre for Medium-Range Weather Forecasts (ECMWF), Météo-France, and Met Office (UKMO)], which have long hindcasts extending back to the mid-twentieth century and are analyzed for their El Niño teleconnections. Increasing greenhouse gasses are not specified in these hindcasts, but given the consistency of ENSO at least over the last half of the twentieth century (Nicholls 2008) this fact should not be a limiting factor for seasonal forecast models. These forecast runs are included in this study to provide context regarding how well we can expect the global coupled models used for climate change to capture El Niño and its teleconnections. These forecast runs have the benefit of being initialized with observed ocean conditions, and thus should be expected to capture the strength and spatial pattern of El Niño as well as or better than free-running CGCMs.
- Nine CMIP3 coupled climate change models selected and grouped according to their twentieth-century ENSO characteristics (based on the analysis of AchutaRao and Sperber 2006):
  - too-weak ENSO variability—Canadian Centre for Climate Modelling and Analysis (CCCma); Goddard Institute for Space Studies Model E-R (GISS-ER); Model for Interdisciplinary Research on Climate 3.2, medium-resolution version [MIROC3.2(medres)];
  - about right ENSO variability—Community Climate System Model, version 3 (CCSM3); third climate configuration of the Met Office Unified Model (HadCM3); Geophysical Fluid Dynamics Laboratory, version 2.0 (GFDL 2.0); and
  - too-strong ENSO variability—Centre National de Recherches Météorologiques (CNRM); ECHAM5; GFDL 2.1.

  These three groups are hereafter referred to as weak, moderate, and strong, respectively. For the groups of models labeled moderate and strong according to their reproduction of El Niño variability, most of these models were also deemed as most realistic according to their representation of tropical Pacific climatology (Guilyardi 2006; 5 out of the 6), and their coupled air–sea variability characteristics (van Oldenborgh et al. 2005b; 4 out of 6).

For the twenty-first-century climate, the A2 Special Report on Emissions Scenario (SRES) projection is chosen for the nine climate change models listed above, as this defines the current worst case envisioned for increased greenhouse gas concentrations. Given that precipitation changes are more subtle than temperature changes, stronger forcing allows for easier detection.

Table 1 provides a list of all coupled climate models and the number of ensemble members for the twentieth

TABLE 1. Coupled climate models and number of ensemble members for the twentieth- and twenty-first-century simulations used in this study.

Modeling group	Acronym	Twentieth-century members	Twenty-first-century members
European Centre for Medium-Range Weather Forecasts	ECMWF	9	—
Centre National de Recherches Météorologiques	Météo-France	9	—
Met Office	UKMO	9	—
	DEMETER group	27	—
Center for Climate System Research (The University of Tokyo), National Institute for Environmental Studies, and Frontier Research Center for Global Change [Japan Agency for Marine-Earth Science and Technology (JAMSTEC)]	MIROC3.2(medres)	3	3
Canadian Centre for Climate Modeling and Analysis	CCCma	5	5
Goddard Institute for Space Studies [National Aeronautics and Space Administration (NASA)]	GISS-ER	9	1
	Weak group	17	9
National Center for Atmospheric Research	CCSM3	8	5
Geophysical Fluid Dynamics Laboratory [National Oceanic and Atmospheric Administration (NOAA)]	GFDL 2.0	3	1
Hadley Centre for Climate Prediction and Research (Met Office)	HadCM3	2	1
	Moderate group	13	7
Centre National de Recherches Météorologiques (Météo-France)	CNRM	1	1
Max Plank Institute for Meteorology	ECHAM5	4	3
Geophysical Fluid Dynamics Laboratory (NOAA)	GFDL 2.1	3	1
	Strong group	8	5

and twenty-first centuries used in the study. The twentieth-century analysis of El Niño teleconnections covers the period from 1959 to 2001, which is the common period of data availability for both seasonal forecast and climate change models. The Climatic Research Unit–University of East Anglia (CRU–UEA) TS2.1 (Mitchell and Jones 2005) is used as the observational precipitation dataset. Both climate model and observed precipitation have been interpolated to a common regular $2.5° \times 2.5°$ grid. The analyses presented here focus on the boreal winter [December–February (DJF)] season, representing the observed peak season for El Niño, and the boreal summer [June–August (JJA)] season when El Niño events typically evolve. Because the seasonality often determines the relevance of El Niño impacts, particularly for precipitation, by examining only specific seasons some regional impacts might not be represented within this study.

The analysis focuses on tropical land (30°N–30°S) and uses a simple meteorological interpretation of drought: below-normal precipitation based on a threshold of seasonally standardized precipitation. No universal definition for drought exists. For agricultural drought, the primary concern is soil moisture, which is also strongly impacted by evaporation as well as details of snowmelt and soil characteristics (e.g., Wang 2005). For hydrological drought, evaporative changes due to temperature are again important as is water demand and even the year-to-year persistence characteristics of the precipitation (e.g., McCabe and Wolock 2007). Even a simple meteorological definition will have its shortcomings. The value of 0.3 standard deviations of the standardized precipitation has been chosen to define the drought threshold because this value approximates the expected standard error following a single-sample z test in a composite of 11 cases (i.e., 11 El Niño events as explained below) drawn from standardized data. Therefore, regions with standardized precipitation anomalies less than or equal to -0.3 are considered to be under drought conditions. The results are consistent using stricter criteria for delimiting drought, which will be illustrated in section 3b when investigating drought spatial extent. Lyon (2004) showed similar consistency in results using differing levels of drought severity.

To investigate tropical droughts associated with El Niño during the twentieth century, composites of standardized precipitation anomalies have been constructed (Fig. 1). The observed composite for DJF (Fig. 1a) is given by the mean standardized precipitation anomalies for the 11 years (1963/64, 1965/66, 1968/69, 1972/73, 1977/78, 1982/83, 1986/87, 1987/88, 1991/92, 1994/95, and 1997/98) classified as El Niño events. El Niño classification is determined by the Niño-3.4 index (mean SST anomaly in the equatorial Pacific region between 5°N and 5°S and 120° and 170°W) falling in the upper quartile of the observed distribution over the common period

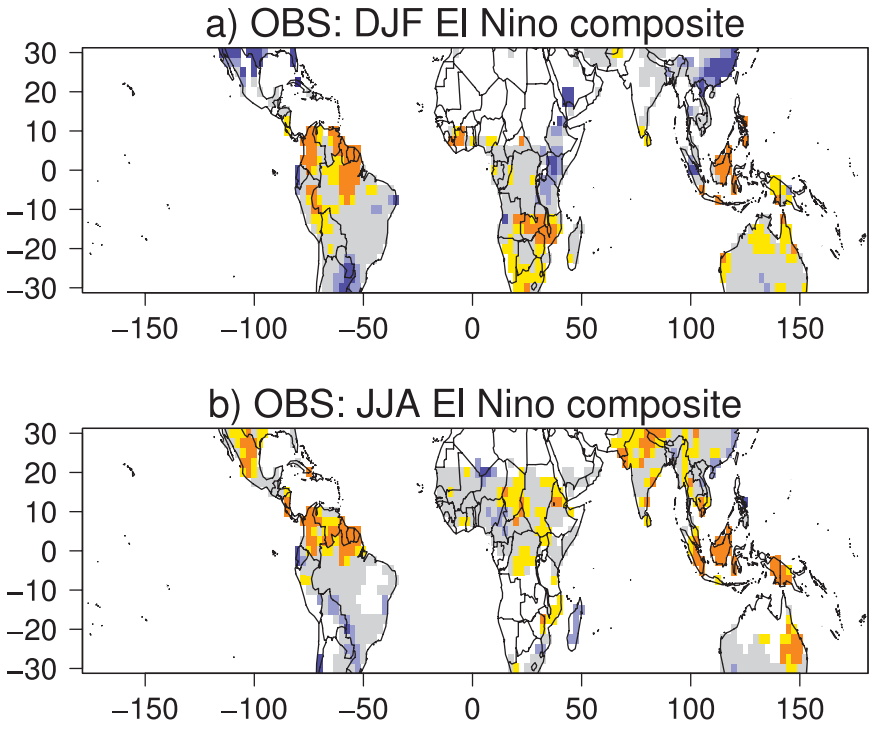

FIG. 1. Observed standardized precipitation anomaly El Niño composites for the twentieth century. (a) DJF composite; (b) JJA composite.

1959–2001. The Niño-3.4 index is chosen because it is a standard and straightforward measure previously shown to correlate most strongly to remote worldwide climate anomalies (Barnston et al. 1997), which is currently used as the primary measure communicated in ENSO monitoring and prediction. Similarly, the observed composite for the JJA standardized precipitation anomalies also includes 11 years (1963, 1965, 1969, 1972, 1982, 1987, 1991, 1992, 1993, 1994, and 1997). Regions with less than 30 mm seasonal precipitation are considered to either be deserts or be experiencing the dry season and are masked out. As previously documented (Ropelewski and Halpert 1987; Mason and Goddard 2001), El Niño events typically lead to negative precipitation anomalies during DJF over northern South America and parts of Indonesia, southern Africa, and north Australia (Fig. 1a). Indonesia, India, northern South America, and much of Central America experience negative precipitation anomalies during JJA of El Niño events (Fig. 1b).

3. El Niño in the twentieth and twenty-first centuries

For the climate change models, an approach similar to that used for the observational Niño-3.4 data is used to delimit El Niño conditions; the upper quartile of the model Niño-3.4 time series determines the El Niño years in each simulation run (i.e., each ensemble member) of each model after carefully removing the effect of temperature trends in the model projections. The temperature trend effect is minimized by computing anomalies relative to a moving 30-year climatological period preceding the year under consideration, consistent with what might be done in real-time forecasting. The upper quartile of Niño-3.4 index that delimits an El Niño event is determined using the preceding 30-year climatological period. The use of a 30-year periods aligns with the World Meteorological Organization (WMO) recommendation, which currently advises the use of the period from 1971 to 2000 as the climatological period for computing climate anomalies.

The standardized precipitation anomalies incorporating the long-term mean and standard deviation have also been produced by computing the climatology from the 30 years of data prior to the year being considered. Figure 2 shows twentieth-century El Niño standardized precipitation anomaly composites for the 9 CMIP3 models investigated for both DJF (first three rows) and JJA (last three rows). Table 2 shows the corresponding standardized precipitation anomaly El Niño composite pattern correlation for each model. The number of

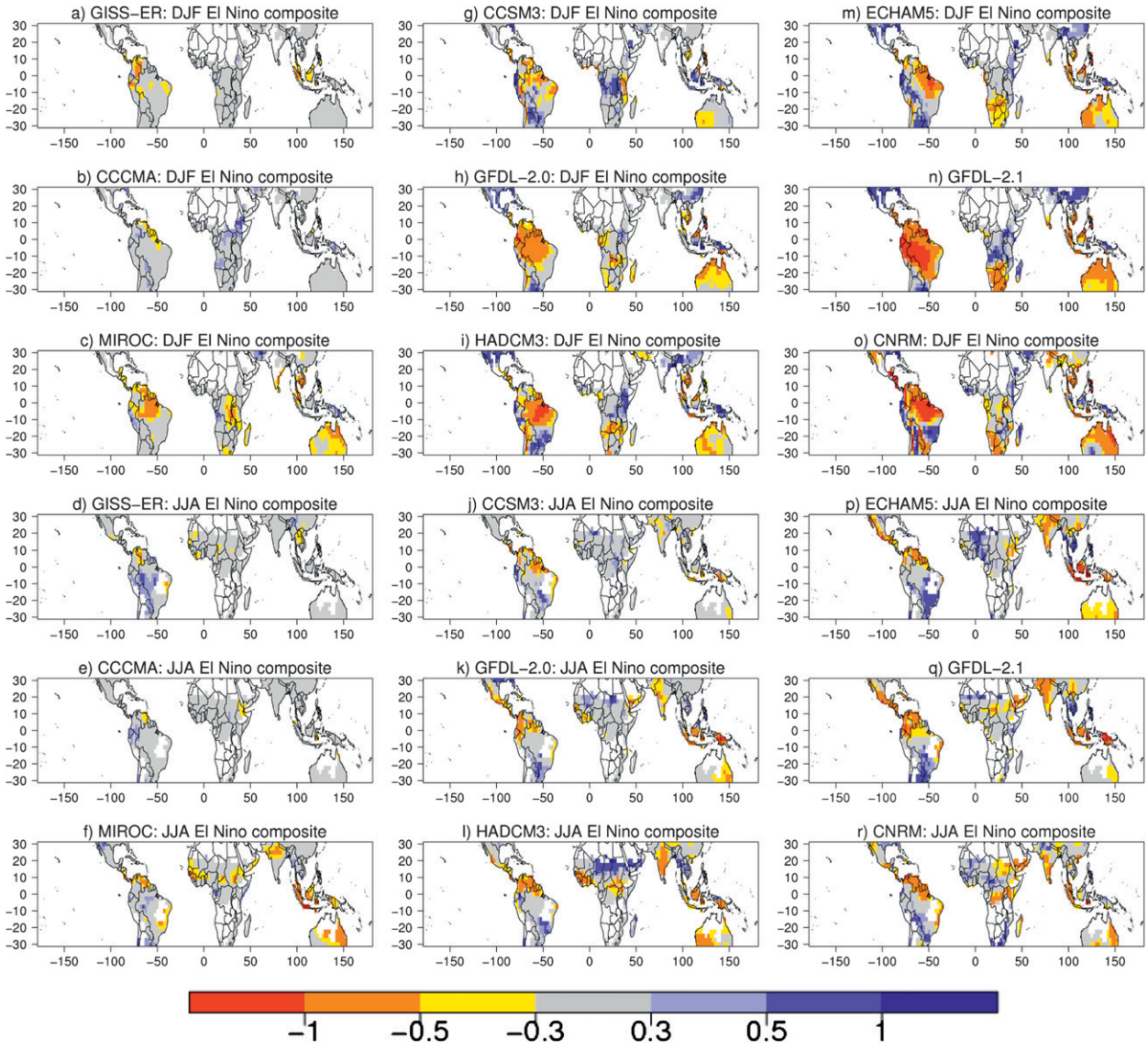

FIG. 2. Standardized precipitation anomaly El Niño composites for the twentieth century for the nine coupled climate change models investigated. (a)–(c) Weak models for DJF. (g)–(i) Moderate models for DJF. (m)–(o) Strong models for DJF. (d)–(f) Weak models for JJA. (j)–(l) Moderate models for JJA. (p)–(r) Strong models for JJA.

events in the composites varies among models as illustrated in Table 3. The average number of El Niño events for each model (values in brackets in Table 3) is close to the observed number of events (11) both in DJF and JJA for nearly all models. All the weak models (first column in Fig. 2) have weak teleconnections and (except CCCma in JJA) and statistically insignificant pattern correlations (Table 2) at the 5% level. Pattern correlation significance has been tested using 500 random composite samples of 11 twentieth-century model fields generated using a bootstrap resampling procedure with replacement. The ranked pattern correlations of the 500 composites, computed against the observed composite (Fig. 1), determine the statistical significance. Values of Table 2 falling outside the 95% confidence interval are label as statistically significant at the 5% level. Table 2 also shows the magnitude of the composite Niño-3.4 index in the twentieth century for all models, which illustrates how the strength of ENSO SST composites varies across different groups of models. For comparison, the observed composite Niño-3.4 index for DJF and JJA are 1.20 and 0.84, respectively.

Among the moderate and strong El Niño models, those that were judged to exhibit realistic SST variability—namely, GFDL 2.0, GFDL 2.1, HadCM3, and ECHAM5 (van Oldenborgh et al. 2005b)—all also exhibit the most

TABLE 2. Standardized precipitation anomaly El Niño composite pattern correlation (PC) and magnitude of the composite Niño-3.4 index for the twentieth century. For comparison, the observed composite Niño-3.4 index for DJF and JJA are 1.20 and 0.84, respectively. The symbol * indicates statistically significant pattern correlation at the 5% level. See text for additional explanation.

	DJF		JJA	
Acronym	PC	Composite Niño-3.4 index	PC	Composite Niño-3.4 index
ECMWF	0.62*	1.15	0.43*	0.86
Météo-France	0.51*	1.04	0.44*	0.68
UKMO	0.64*	1.40	0.48*	1.12
DEMETER group	0.69*	—	0.50*	—
MIROC3.2(medres)	0.25	0.61	0.33	0.62
CCCma	0.29	0.57	0.25*	0.38
GISS-ER	0.22	0.26	0.17	0.25
Weak group	0.36*	—	0.30*	—
CCSM3	0.15	1.11	0.33*	0.79
GFDL 2.0	0.57*	1.29	0.42*	1.11
HadCM3	0.46*	1.08	0.28	0.93
Moderate group	0.38*	—	0.42*	—
CNRM	0.23*	1.80	0.35*	0.89
ECHAM5	0.50*	1.68	0.48*	1.33
GFDL 2.1	0.54*	2.26	0.49*	1.76
Strong group	0.60*	—	0.54*	—

TABLE 3. Total number of El Niño events during the 20th Century used for producing the composites of Fig. 2 for the nine coupled climate change models among all available ensemble members of each model. The values in brackets are the average number of El Niño events during the 20th Century among all available ensemble members as indicated in Table 1. For comparison, the observed number of El Niño events during the 20th Century is 11 for both DJF and JJA.

Acronym	DJF	JJA
MIROC3.2(medres)	30 (10)	29 (9.7)
CCCMA	71 (14.2)	79 (15.8)
GISS-ER	94 (10.4)	108 (12)
CCSM3	97 (12.1)	79 (9.9)
GFDL-2.0	34 (11.3)	33 (11)
HADCM3	25 (12.5)	23 (11.5)
CNRM	10 (10)	11 (11)
ECHAM5	40 (10)	38 (9.5)
GFDL-2.1	36 (12)	37 (12.3)

realistic teleconnections. The El Niño composite precipitation anomalies for these models (except in HadCM3 in JJA) correlate significantly with the observed composite at the 5% level (Table 2). Consistent with the results of Lyon (2004), Fig. 2 shows a clear relationship between the magnitude of regional El Niño precipitation teleconnections and the magnitude of El Niño variability as represented in each group of models. Such a relationship between the strength of El Niño and local precipitation response might be expected in a single model. The existence of this relationship across models highlights the concern for possible increasingly strong El Niño events in the future.

Prior to examining changes in El Niño teleconnections in the twenty-first century, we first examine changes in El Niño itself. Solomon et al. (2007) suggest that the models are split in their tendency for more or less El Niño variability in the future, but that the trends in tropical Pacific SST most often correlate positively with El Niño (Meehl et al. 2007, cf. Figure 10.16). Although this is consistent with the studies cited earlier (van Oldenborgh et al. 2005b; Collins et al. 2005; Merryfield 2006), the highly condensed nature of the IPCC summary on ENSO falls short in indicating what the models are actually indicating with regard to El Niño and gives the impression that we will either have more El Niño events in the future, or that trends in the mean climate are likely to reflect persistent El Niño conditions.

To what degree can significant conclusions be drawn on the change in El Niño characteristics from the limited number of cases available for a phenomenon that contains large interevent variability? Subtle differences leaning toward more or less El Niño variability in the future could be influenced by the period analyzed (Knutson et al. 1997) or by a particular outlier ensemble member. Here, each model's ensemble member is treated individually, as any single ensemble member could represent a realization of nature. Recall that the designation of an El Niño even in the CMIP3 models throughout the last half of the twentieth century and through the twenty-first century rests on the climatology and event thresholds of the previous 30 years. For each ensemble member of a particular model, the magnitude of El Niño events over the twentieth or twenty-first centuries constitute sample populations that may or may not be drawn from the same distribution. For investigating possible changes in the magnitude of El Niño we apply the Wilcoxon rank sum test (Wilcoxon 1945), which is equivalent to the Mann–Whitney U test (Mann and Whitney 1947) testing the null hypothesis that the two populations are drawn from identical continuous distributions with equal medians. The significance level (p value) at which the null hypothesis may be rejected is plotted (Fig. 3a) for all possible pairs of DJF ensemble members from the twentieth and twenty-first centuries compared to one another (black diamonds) and between different DJF ensemble members within the twentieth century (gray circles). Any point below the 0.05 p value line indicates that the difference in the medians of the two samples is statistically significant at the 5% level. One must consider the range of values from pairing the different ensemble members within a given century in

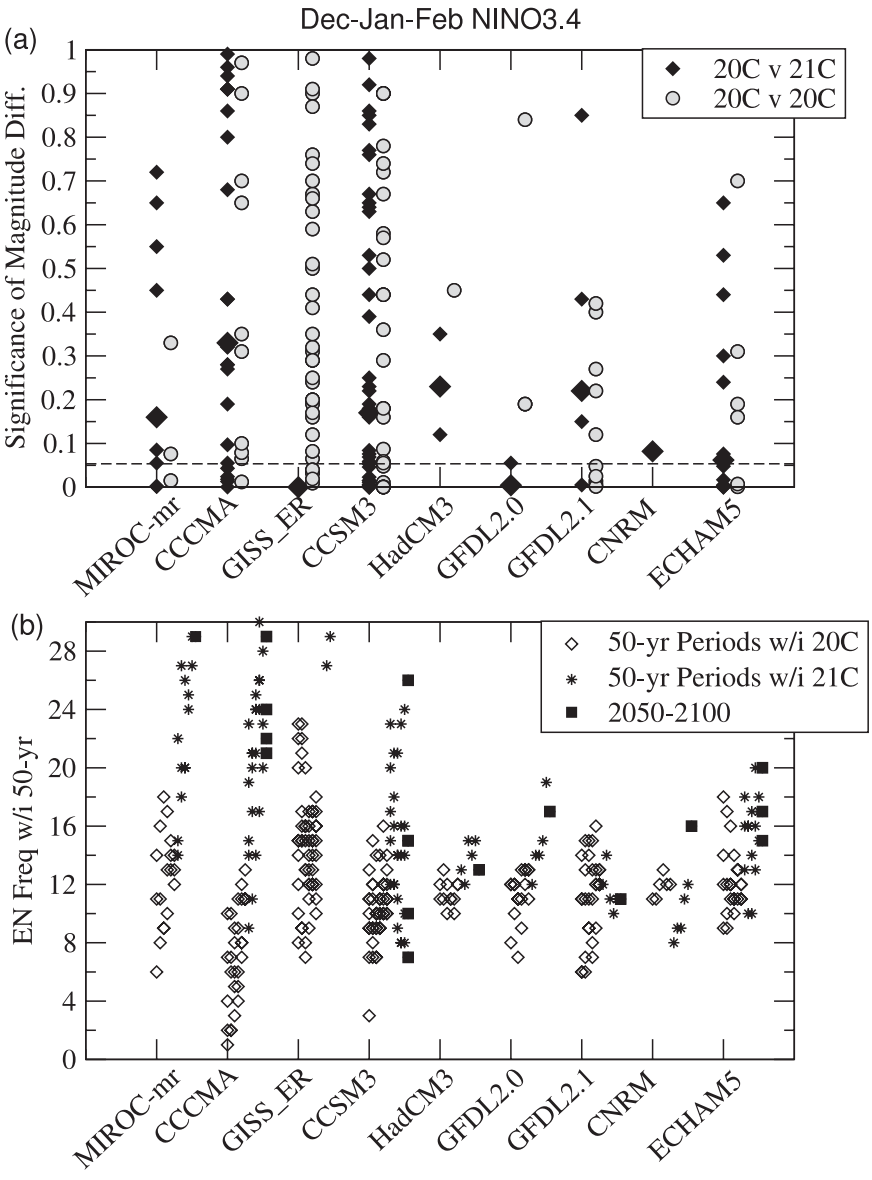

FIG. 3. Robustness of changes in El Niño magnitude and frequency. (a) Significance level (i.e., p value) of Wilcoxon rank sum test for DJF Niño-3.4 index equal medians comparing all possible pairs of samples from individual ensemble members of El Niño magnitude within the twentieth century (gray circles) and between the twentieth and twenty-first centuries (black diamonds, median value marked with larger diamond); (b) frequency of El Niño events within 50-year periods during the twentieth century (open diamonds) and twenty-first century (black stars). See text for additional information. Final 50-year period of twenty-first century highlighted with black squares.

addition to the few cases suggesting significant differences between the twentieth and the twenty-first centuries. Even within the twentieth century, it is possible to show statistically significant differences in the magnitude of El Niño events at the 5% level, though the two runs were subject to identical external forcing. The importance of larger ensemble availability is obvious for both the historical simulations and the future projections, especially for drawing conclusions on changes in variability.

Small ensemble sizes similarly limit examination of change in the frequency of El Niño events, making statistical tests much more difficult. One can get a sense of how El Niño frequency in DJF is projected to change in the models and how the paucity of ensemble members clouds definitive conclusions by simply looking at the

number of El Niño events in 50-year chunks within the twentieth and twenty-first centuries (Fig. 3b). Six overlapping 50-year chunks were used for each century: 1901–50, 1911–60, 1921–70, 1931–80, 1941–90, and 1951–2000, and similarly for the twenty-first century. For the models that do not contain El Niño events (e.g., GISS-ER), increased frequency results merely from the fact that the tropical Pacific warms because of the external forcing, so going forward SSTs appear increasingly warmer than the previous 30 years. For models that do contain El Niño events, the frequency of events for the twenty-first century typically resides within the range seen during the twentieth century, or approximately 1 event per 4 years. Cases do exist showing frequencies not experienced in the twentieth century, but no monotonic increases through the twenty-first century are found. The importance of multiple ensemble projections is clearly demonstrated by CCSM3, which provides five ensemble members for the twenty-first century. Quite different conclusions on the future of El Niño frequency could be drawn if one had only the single member that ended the twenty-first century with unprecedented El Niño frequency compared to the situation in which one had only the single member that ended with a frequency close to the twentieth-century low. Although some slight tendency toward possible small increases of El Niño frequency can be seen in these models, no robust conclusions can be drawn other than that discerning such a shift in the observed record will defy attribution to global warming. This conclusion indicates that, given the limited sampling available from both the observed record and the climate model projections, the characteristics of El Niño events through the twenty-first century are currently projected to remain consistent with those of the twentieth century. Similar conclusions exist for El Niño strength and frequency changes for JJA (not shown).

4. Tropical El Niño teleconnections in the twenty-first century in coupled model projections

a. Spatial patterns and magnitude

The previous section has shown that the strength of El Niño events is not projected to change in the twenty-first century. The analysis presented in section 3 allows a more qualified basis for that statement than given in previous studies because that statement is confirmed by each and every of the individual models, rather than as the apparent disagreement of the set of models. However, the background mean climate against which El Niño events evolve is changing. To what extent will the changes in tropical mean climate modify El Niño teleconnections? And, does the strength or frequency of ENSO variability as represented by a particular model influence the character of the climate change precipitation response in the model?

The results presented in section 3 show that, across climate models and as previously shown by Lyon (2004) using observations, the strength of tropical precipitation teleconnections scales with the strength of El Niño. Therefore, tropical precipitation will henceforth be further composited across models in the weak, moderate, and strong El Niño groups to focus the common features within the groups and highlight differences due to different representation of El Niño (Figs. 4 and 5). The superiority of pattern correlation in the teleconnections among the DEMETER models particularly in DJF (Table 2) is related to a more realistic spatial pattern of El Niño afforded by ocean initialization compared to the free-running climate change simulations (Misra et al. 2008) just as, within the CMIP3 models, those with more realistic representation of ENSO SST variability contained better representation of the tropical teleconnection patterns. As the magnitude of the El Niño–related precipitation anomalies scales with the strength of El Niño, the moderate group yields the most similarity to the seasonal forecast DEMETER composite (Figs. 4b–d and 5b–d).

Comparison of the twenty-first-century El Niño standardized precipitation anomaly composites (Figs. 4e–g) with the twentieth-century composites (Figs. 4b–d) for DJF reveals that neither the magnitude of the anomalies nor the spatial patterns are projected to change substantially in the twenty-first century in any of the three groups of models, despite the fact that the climate mean state changes. Similar results are found for JJA (Fig. 5). Statistical significance of the differences has been assessed by generating 1000 random samples using a simple bootstrap resampling procedure with replacement for each group of models for the twentieth and twenty-first centuries. The statistical significance for the difference between the twentieth- and twenty-first-century composites depends on whether the 95% confidence intervals for the twentieth- and twenty-first-century composites overlap. This procedure has been applied at each grid point independently. For nearly all land areas no differences have been detected at the 5% level (i.e., no changes have been identified between the twentieth- and twenty-first-century El Niño composite projections) (not shown). The number of grid points differing at the 5% level or better is less than that expected by chance.

Examination of teleconnection differences in Figs. 4 and 5 is based on standardized anomalies. However, there may be changes in precipitation variability (i.e., the standard deviation) that would not appear in the

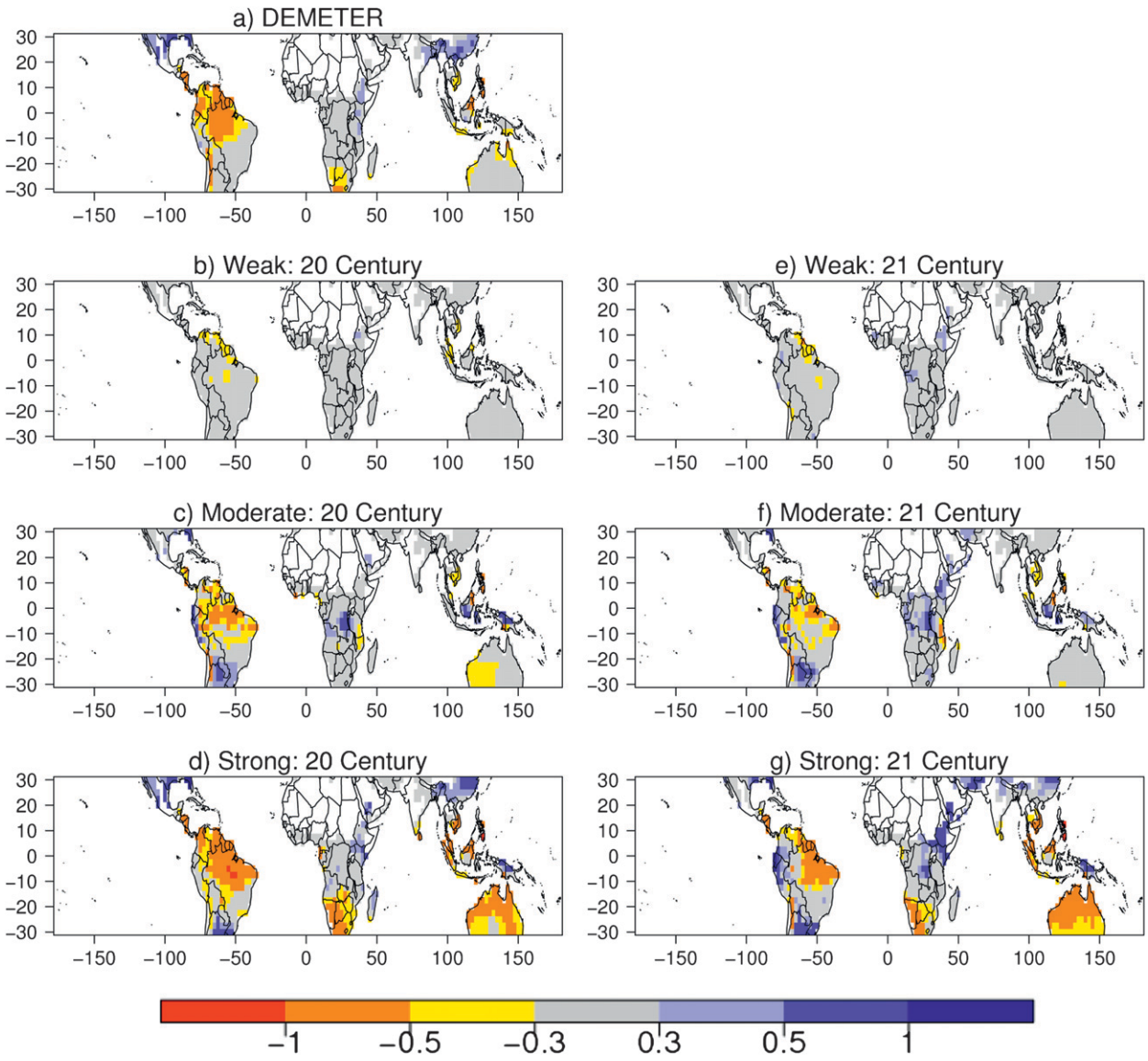

FIG. 4. DJF standardized precipitation anomaly El Niño composites for (a) the DEMETER group, (b) weak group, (c) moderate group, and (d) strong group during the twentieth century. Standardized precipitation anomaly El Niño composites for the (e) weak, (f) moderate, and (g) strong groups during the twenty-first century.

relative standardized precipitation anomalies. Thus the same analysis of changes in El Niño teleconnections is applied to quantitative precipitation anomaly composites. The observed actual precipitation anomaly El Niño composite in mm day^{-1} (Fig. 6a) shows a similar pattern to the observed standardized precipitation anomaly composite (Fig. 1a), as do the model groups (Figs. 6b–g compared to Figs. 4b–d) in accordance with the standardized precipitation anomaly composites (Figs. 4b–g), actual precipitation anomaly composites (Figs. 6b–g) for all three groups of climate change models do not show marked differences between the twentieth- and twenty-first-century El Niño composite projections. Therefore, in both the relative and absolute sense no differences exist between El Niño composite projections for the twentieth and twenty-first centuries. Similar results have been found for JJA (not shown).

b. Range of variability and spatial extent

Figure 7 illustrates, using box plots (also known as box and whisker diagrams), the range of variability between El Niño composites for all ensemble members of each group of models for four regions where El Niño events typically lead to reduced precipitation in DJF: northern

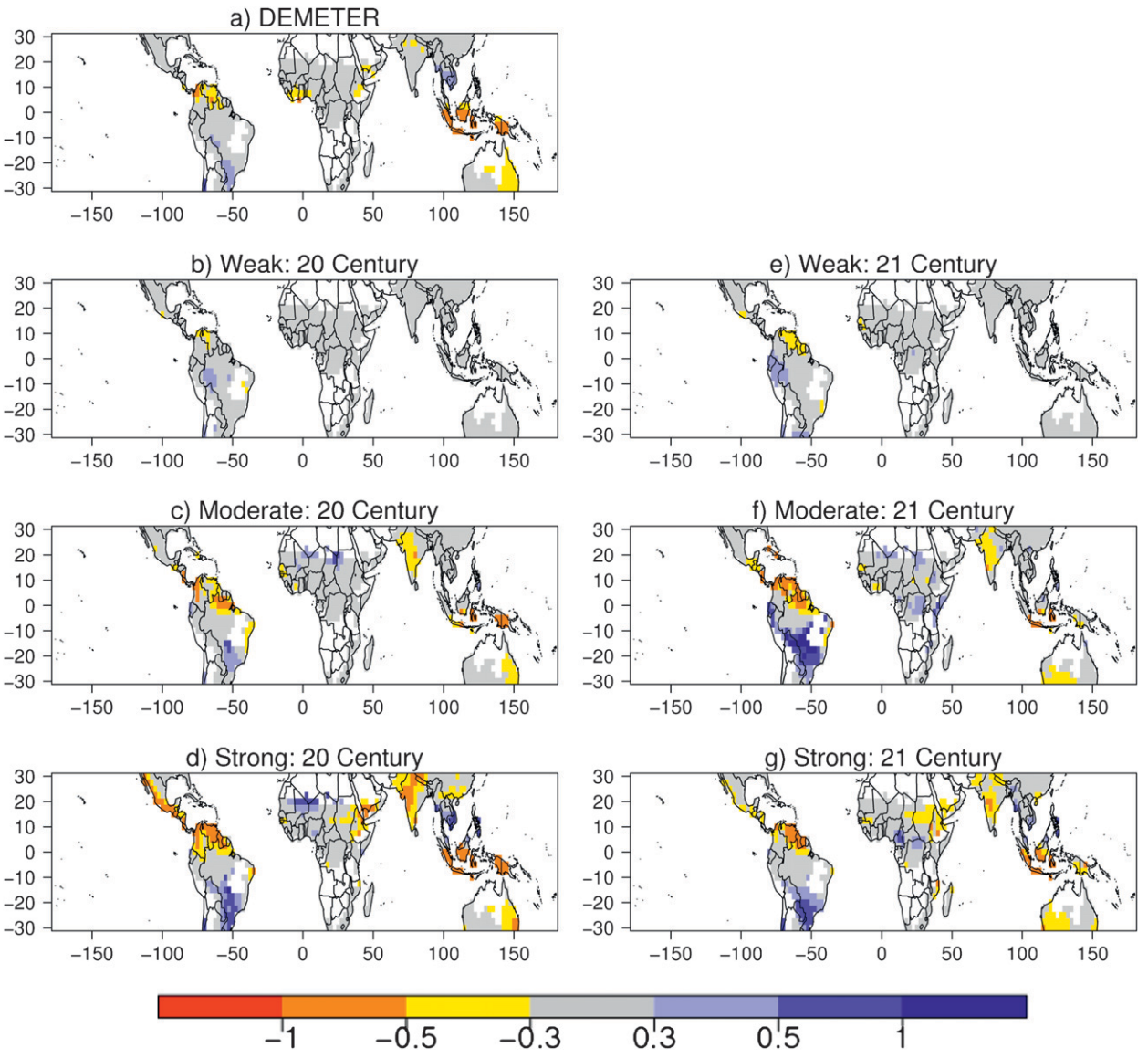

FIG. 5. Same as Fig. 4, but for JJA.

South America (10°N–10°S, 75–50°W) (Fig. 7a), southern Africa (20–30°S, 10–40°E) (Fig. 7b), Indonesia (2.5–7.5°S, 110–120°E) (Fig. 7c), and north Australia (10–20°S, 130–150°E) (Fig. 7d). The box plots shown in Fig. 7 are constructed using the standardized precipitation anomaly composites.

The central gray box of the DEMETER seasonal forecast model group incorporates the observed standardized precipitation anomaly composite (horizontal dashed line) for northern South America (Fig. 7a), southern Africa (Fig. 7b), and north Australia regions (Fig. 7d). The mean (black dot) and median (thick horizontal line) values for the DEMETER group over these three regions are also close to the observed standardized precipitation anomaly, indicating good performance in predicting the observed standardized precipitation anomaly. Over Indonesia (Fig. 7c) the DEMETER group shows a large spread, indicating high prediction uncertainty or large intraevent variability, but the ensemble range of values does contain the observed anomaly. The ensemble range of values for nearly all groups of models shows the ability of theses models to cover the observed anomaly during the twentieth century. The only two exceptions are the weak group of models for southern Africa (Fig. 7b) and the moderate group of models for Indonesia (Fig. 7c), where the range of the ensemble does not cover the observed value. The comparison of the box plots for each group of climate change

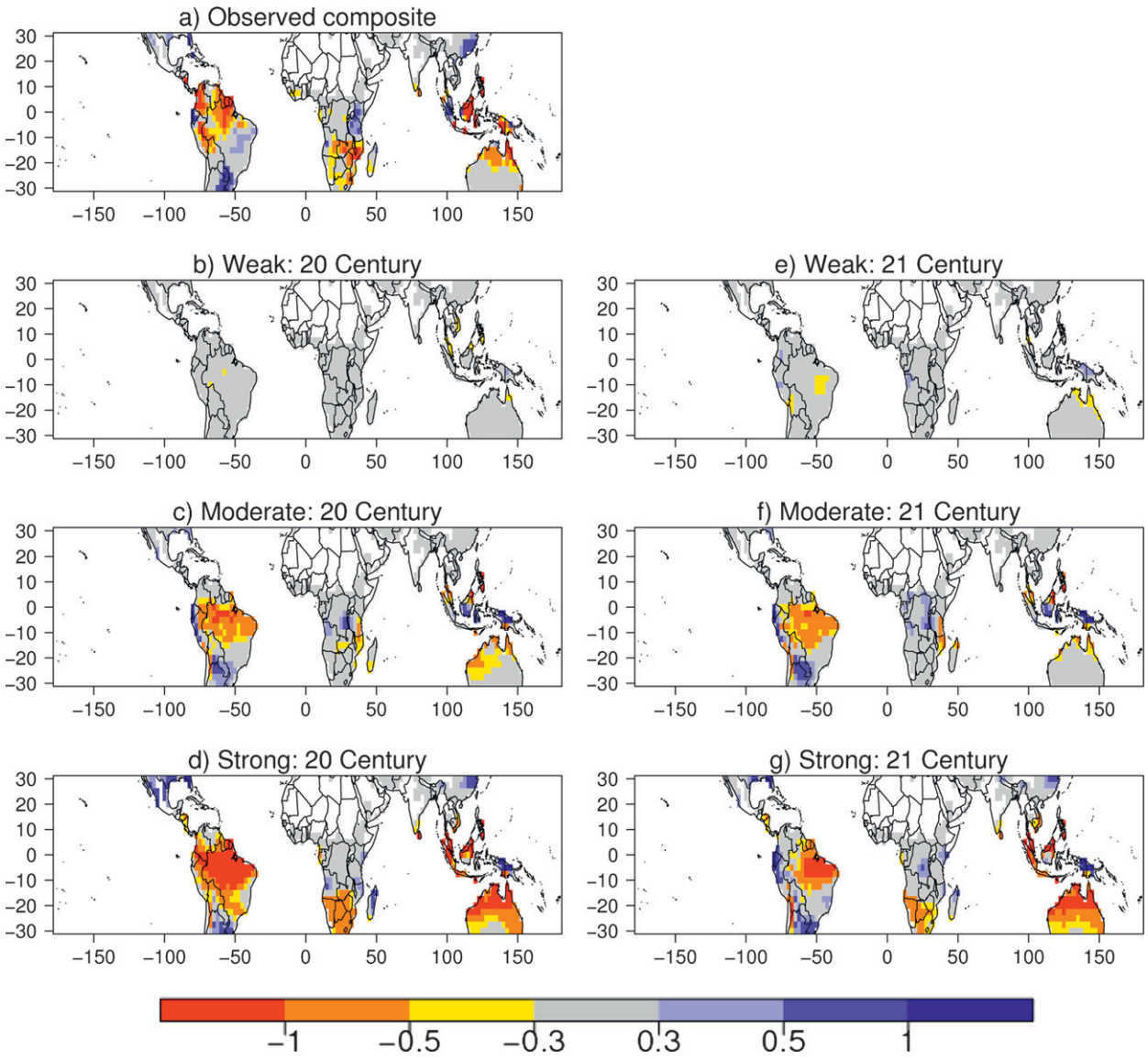

FIG. 6. (a) Observed DJF precipitation anomaly El Niño composite. DJF precipitation anomaly El Niño composites for the (b) weak, (c) moderate, and (d) strong groups during the twentieth century. DJF precipitation anomaly El Niño composites for the (e) weak, (f) moderate, and (g) strong groups during the twenty-first century. Precipitation anomalies are expressed in millimeters per day.

models shows a consistent overlap between the range of values projected for the twentieth and twenty-first centuries. In accordance with Fig. 4, this result supports the finding of no discernable change between the twentieth- and twenty-first-century El Niño projections for northern South America, southern Africa, Indonesia, and north Australia.

Figure 8 shows El Niño standardized precipitation anomaly composite box plots for three regions where El Niño leads to reduced precipitation in JJA: northern South America (10°N–10°S, 75–50°W) (Fig. 8a), Indonesia (2.5–7.5°S, 110–120°E) (Fig. 8b), and east Australia (20–30°S, 140–150°E) (Fig. 8c). Overall, the same features described above for DJF are present in JJA. The main difference compared to DJF is the larger number of model groups with the ensemble range of values unable to cover the observed anomaly during the twentieth century [e.g., the DEMETER and weak group of models for South America (Fig. 8a) and the weak, moderate, and strong group of models for Indonesia (Fig. 8b)].

Another important El Niño feature is the spatial extent of the precipitation anomaly, particularly negative ones (Fig. 9). Box plots are constructed for all ensemble members available for each group of models. The

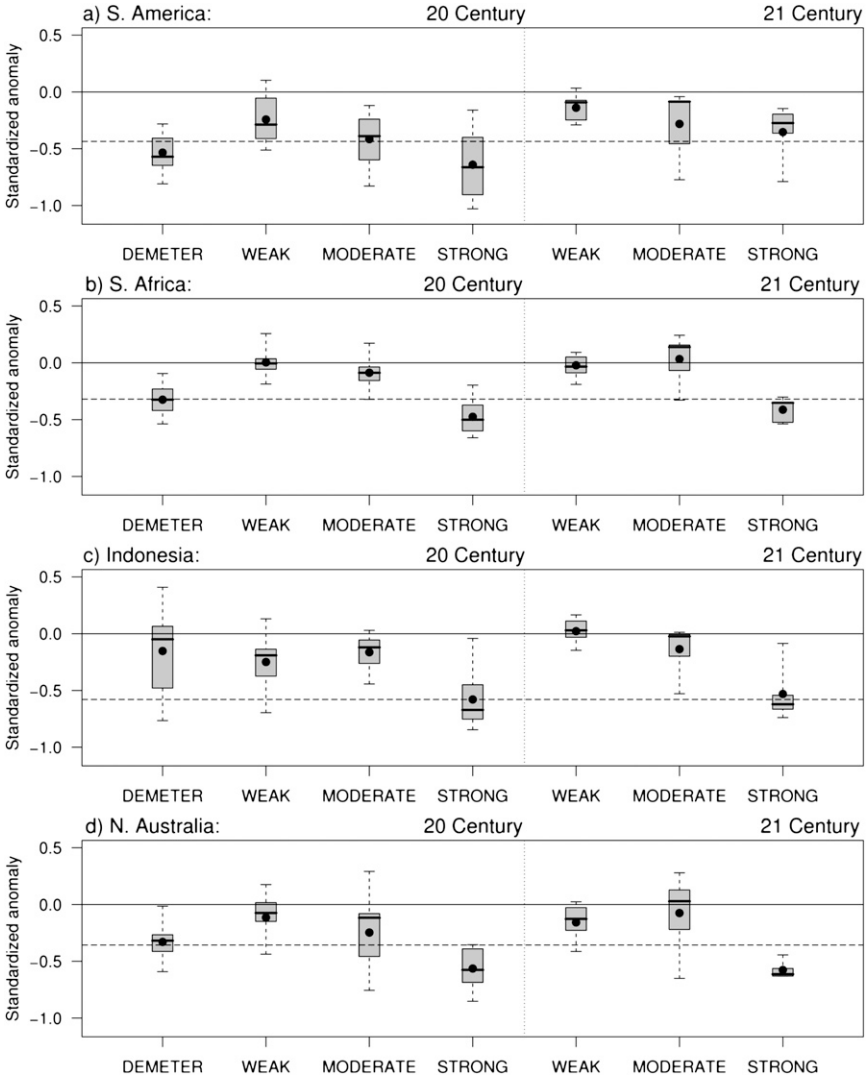

FIG. 7. Box plots of DJF El Niño composites standardized precipitation anomaly for all ensemble members available for the four groups of models investigated. Box plots are shown for four regions: (a) northern South America (10°N–10°S, 75–50°W), (b) southern Africa (20–30°S, 10–40°E), (c) Indonesia (2.5–7.5°S, 110–120°E), and (d) north Australia (10–20°S, 130–150°E). Box plots located to the left (right) of the vertical dotted line are for the twentieth- (twenty-first) century composites. The horizontal dashed line is the observed composite standardized precipitation anomaly in the twentieth century. The central horizontal thick line within the box is the median value among all ensemble members. The box represents the interquartile range. The whiskers are drawn as far as the highest and lowest values of the ensemble. The black dot is the ensemble mean.

DEMETER, weak, and moderate model groups have mean (black dot) and median (thick horizontal line) close to the observed fraction (horizontal dashed line) during the twentieth century, indicating that these two model groups have a good spatial extent of negative anomalies during El Niño years. Ensemble members from the strong El Niño models show a higher fraction of grid points with drought during El Niño than seen in the weak and moderate models. Only DEMETER and weak models do contain the observed fraction within their ensemble range during the twentieth century in DJF (Figs. 9a,b), while for JJA the DEMETER, weak, and moderate models do contain the observed fraction (Figs. 9c,d). All three groups of climate change models suggest a slight reduction in the spatial extent of drought, at both severity levels, compared to the twentieth-century projected fraction. However, the twenty-first-century results are based on far fewer ensemble members than

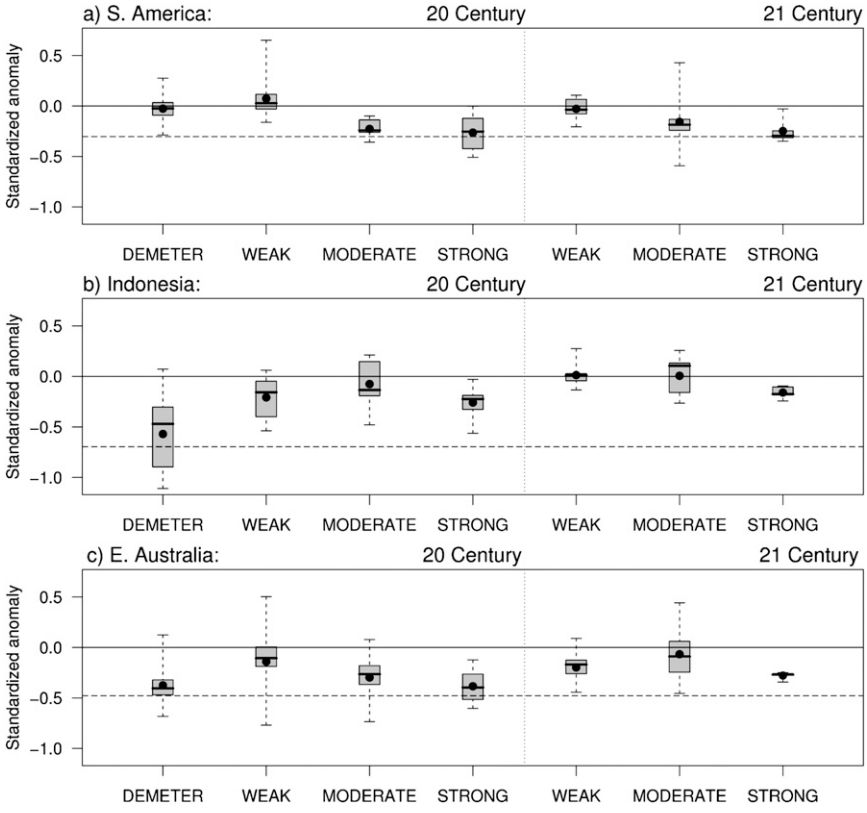

FIG. 8. Box plots of JJA El Niño composites standardized precipitation anomaly for all ensemble members available for the four groups of models investigated. Box plots are shown for three regions: (a) northern South America (10°N–10°S, 75–50°W), (b) Indonesia (2.5–7.5°S, 110–120°E), and (c) east Australia (20–30°S, 140–150°E). Box plots located to the left (right) of the vertical dotted line are for the twentieth- (twenty-first) century composites. The horizontal dashed line is the observed composite standardized precipitation anomaly in the twentieth century. See text for additional explanation.

used for the twentieth century. This sampling issue and the amount of overlap between the two centuries mean that the result of a slight reduction should be interpreted with caution.

5. El Niño–induced drought risk: The intersection between climate variability and change

The climate literature states that climate change projections for many parts of the world depend on how ENSO may change in the future (van Oldenborgh et al. 2005b). Projections have even been called into question because of the limited ability of most climate change models to represent ENSO. Thus, a reasonable question would be: to what extent does the fidelity of ENSO in a coupled model influence the resulting changes in the mean climate? For the tropics, broadly, the ability of a model to represent the dominant aspect of climate variability, namely ENSO, does not control the climate change response. Figure 10 shows the projected change, between the periods 2071–2100 and 1971–2000, in the mean DJF and JJA precipitation from the three climate change model groups. Consistent with the tendency toward a warmer tropics in the twenty-first century (Solomon et al. 2007), all three climate change model groups project increases in tropical precipitation, particularly between 10°N and 10°S (e.g., Held and Soden 2006). The magnitude and broad pattern of the projected precipitation change do not scale with the strength of ENSO in the models. The differences between models within any particular group (not shown) are typically larger than the differences between the groups shown in Fig. 10. Thus changes in mean precipitation within the tropics are largely independent of a model's ENSO characteristics. Even models that have little to no ENSO variability (Figs. 10a,d) produce a change in mean precipitation of similar magnitude and spatial structure to those models with exceedingly strong ENSO variability (Figs. 10c,f).

The intersection of projected changes in mean precipitation and projected El Niño precipitation teleconnections

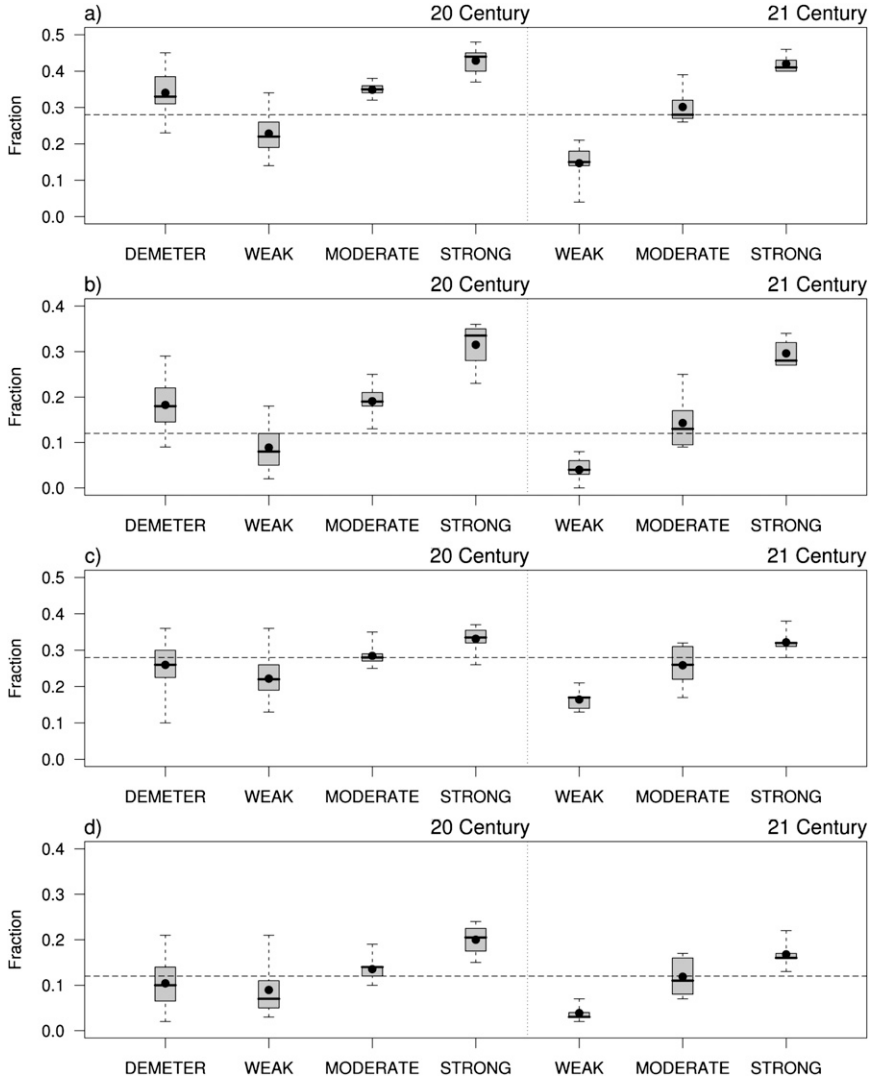

FIG. 9. Box plots for the fraction of land grid points with negative standardized precipitation anomaly El Niño composites for the four groups of models investigated for two drought severity levels: (a) DJF and (c) JJA standardized precipitation anomalies less than 0.3, and (b) DJF and (d) JJA standardized precipitation anomalies less than 0.5. Box plots are constructed using the gridpoint fraction of negative standardized precipitation anomaly composites for all ensemble members for each group of models. Box plots located to the left of the vertical dotted line are for the twentieth-century composites. Box plots located to the right of the vertical dotted line are for the twenty-first-century composites. The horizontal dashed line is the observed fraction of land grid points with negative standardized precipitation anomaly El Niño composite in the twentieth century.

for the twenty-first century can help identify regions where adverse El Niño–related precipitation impacts are likely to decrease or increase in the future. The results presented so far provide supportive evidence that, for the tropics, climate variability and change are largely separable. Therefore, it may be possible to combine, or layer, information from the different time scales (i.e., long-term climate change and short-term climate variability) obtained from different sources. In terms of climate variability, the models project unchanging precipitation teleconnections associated with ENSO. However, that variability is riding on top of a changing mean climate that is attributable to anthropogenic climate change. This means that, even if the climate variability is unchanged, the risks of a predefined event such as drought (i.e., precipitation below a certain value) will change.

Often the average answer from a set of predictions is taken as the net forecast. If a set of forecasts all agree in

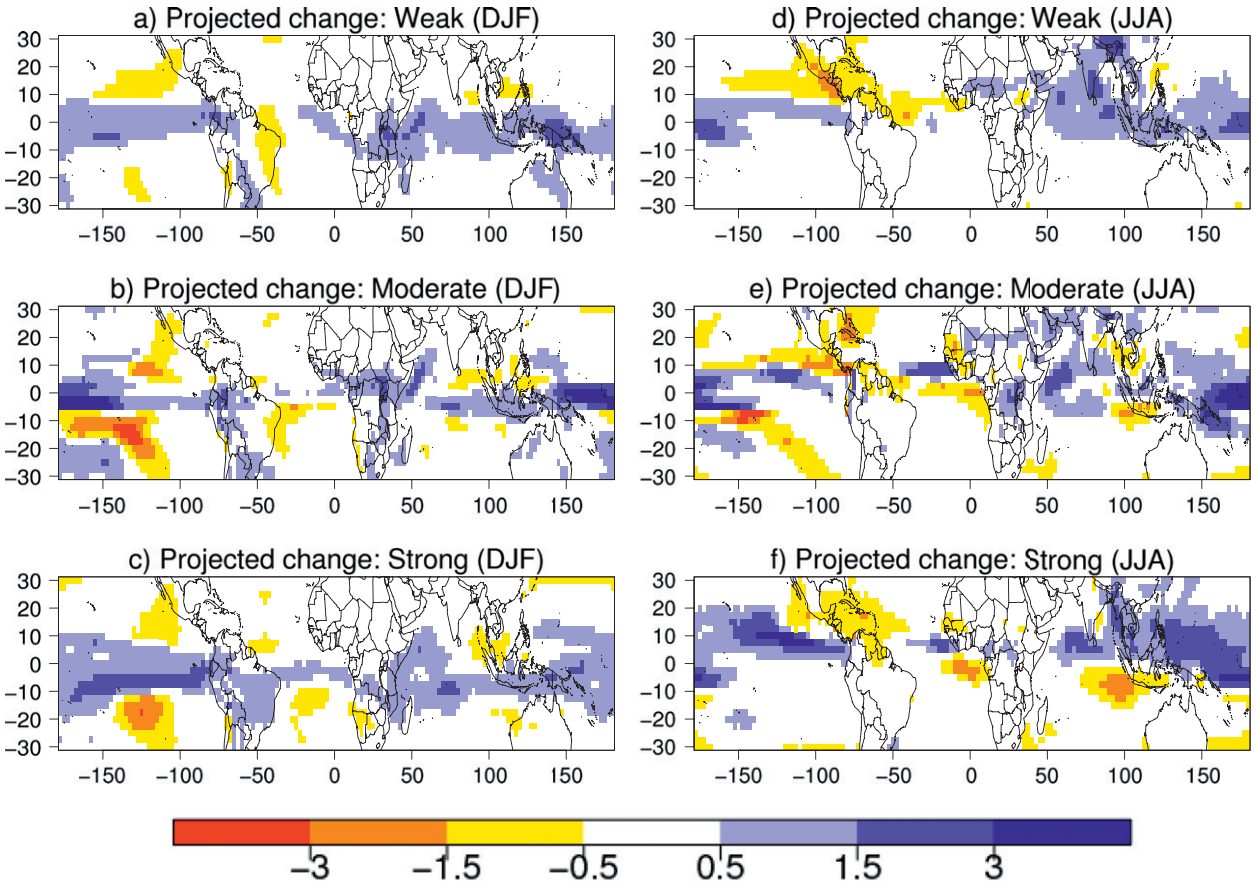

FIG. 10. Difference in (a)–(c) DJF and (d)–(f) JJA mean precipitation anomaly (in mm day^{-1}) between the period 2071–2100 and 1971–2000 simulated by (top) weak, (middle) moderate, and (bottom) strong El Niño groups of climate change models.

predicting no change, the net forecast is for no change. If a set of forecasts all disagree such that their average prediction is no change, it is still commonly interpreted as a net forecast of no change. The two situations are quite different. Both situations exist to some degree in this analysis. For climate variability, the set of models agree in individually predicting no significant change in El Niño strength or magnitude. Furthermore, the models predict no change in the precipitation teleconnections associated with El Niño events. Thus, the observed El Niño teleconnections of the twentieth century can be used to represent those of the twenty-first century. However, climate variability exists in combination with a changing mean climate. For the change in mean climate the models do not always agree at local to regional scales. The main difficulty in dealing with the situation of diverging model predictions is determining which models to trust. If the models were all equally credible, the spread of predictions should contribute to estimating the probabilistic uncertainty of the outcome. The approach taken by the IPCC AR4 (Meehl et al. 2007) is simply to form multimodel averages and possibly to highlight areas where the models agree in the magnitude, or at least the sign, of their twenty-first-century climate change. Similar approaches are adopted here to examine the changing risk of drought or, more specifically, deficient precipitation.

The threshold for drought conditions is defined to be the 30th percentile of the observed precipitation distribution for the last half of the twentieth century based on a fit of the observed values at each point to a gamma distribution. For standardized normally distributed data, the 30th percentile coincides approximately with 0.5 standard deviations below average; for positively skewed precipitation distributions common of semiarid regions the 30th percentile is often close to the −0.3 standard deviations considered in previous sections. This threshold is not necessarily the relevant measure of drought for all locations, and, as mentioned earlier, consideration of only precipitation ignores other variables relevant to drought such as temperature. This example merely illustrates how changing risk of some predetermined

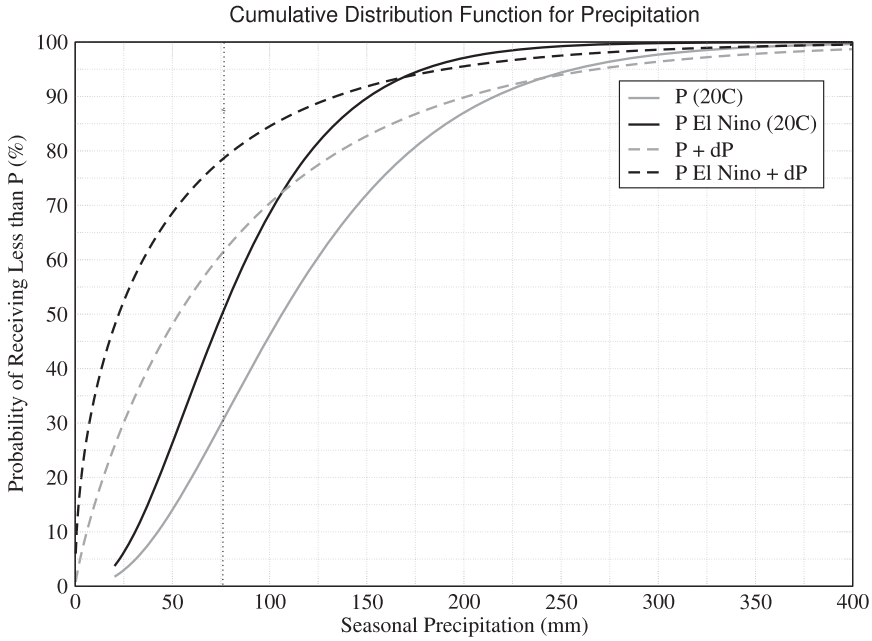

FIG. 11. Cumulative distribution functions for precipitation showing the probability (%) of receiving less than a given amount of precipitation (mm) based on fitting a gamma distribution to observed values at a single grid point. The CDFs for twentieth-century precipitation (solid lines) are drawn both for all years (gray: DJF 1959–2001) and El Niño conditions during that period. Similar curves are presented for the twenty-first-century precipitation by adding the CMIP3 multimodel mean precipitation changes at that location to the observed twentieth-century time series and reestimating the parameters.

quantitative threshold could be assessed with the data available. By construction, the risk of ''drought'' over the last half of the twentieth century is 30%. The quantitative value of how much precipitation is associated with the 30th percentile will vary spatially. In the example shown in Fig. 11, using the data from a single grid point, the threshold for drought is approximately 75 mm of rainfall for the season. To produce probabilistic maps of drought risk during El Niño conditions in the twentieth century, just those 11 observations associated with El Niño conditions are used to fit a gamma distribution. The resulting cumulative distribution function (CDF) permits estimation of the probability of the predefined threshold. In the example (Fig. 11), risk of falling below the drought threshold (75 mm) increases to about 50% during El Niño conditions, or an increase in drought risk of about 20% compared to the twentieth-century climatological risk. Maps of these probabilities during El Niño conditions for DJF and JJA in the twentieth century reiterate the known teleconnection regions (Figs. 12a and 13a; compare with Fig. 1). Masked out regions (Figs. 12a, 13a, and left-hand panels in Figs. 12b–e and 13b–e) indicate climatologically dry areas according to the mean precipitation of the twentieth century as described in section 2.

The risk of drought during El Niño conditions near the end of the twenty-first century (Figs. 12b and 13b) is obtained by layering the climate information of variability (Fig. 1) and change (Fig. 10). The change in mean precipitation is determined from the climate change models by differencing the (1971–2000) and (2071–2100) multimodel mean. The precipitation change is then added to the observed time series, the parameters of the gamma distributions are recalculated, and the probabilities for the predefined threshold are reevaluated. Addition of the projected change effectively shifts the CDF based on the sign of the change. In the example (Fig. 11), the precipitation change is negative, and the probability for receiving less than 75 mm for the season increases climatologically to about 60% and to about 80% during El Niño conditions at the end of the twenty-first century, which translates into a 30% increase in drought risk.

The question of confidence in the multimodel mean precipitation changes remains. A number of criteria are considered to illustrate the sensitivity of the results to how one determines confidence. If confidence cannot be established at a location, the assumption is that the mean precipitation change cannot be determined, and no change is imposed on the characteristics of the twentieth-century time series for use in calculating twenty-first-century risk

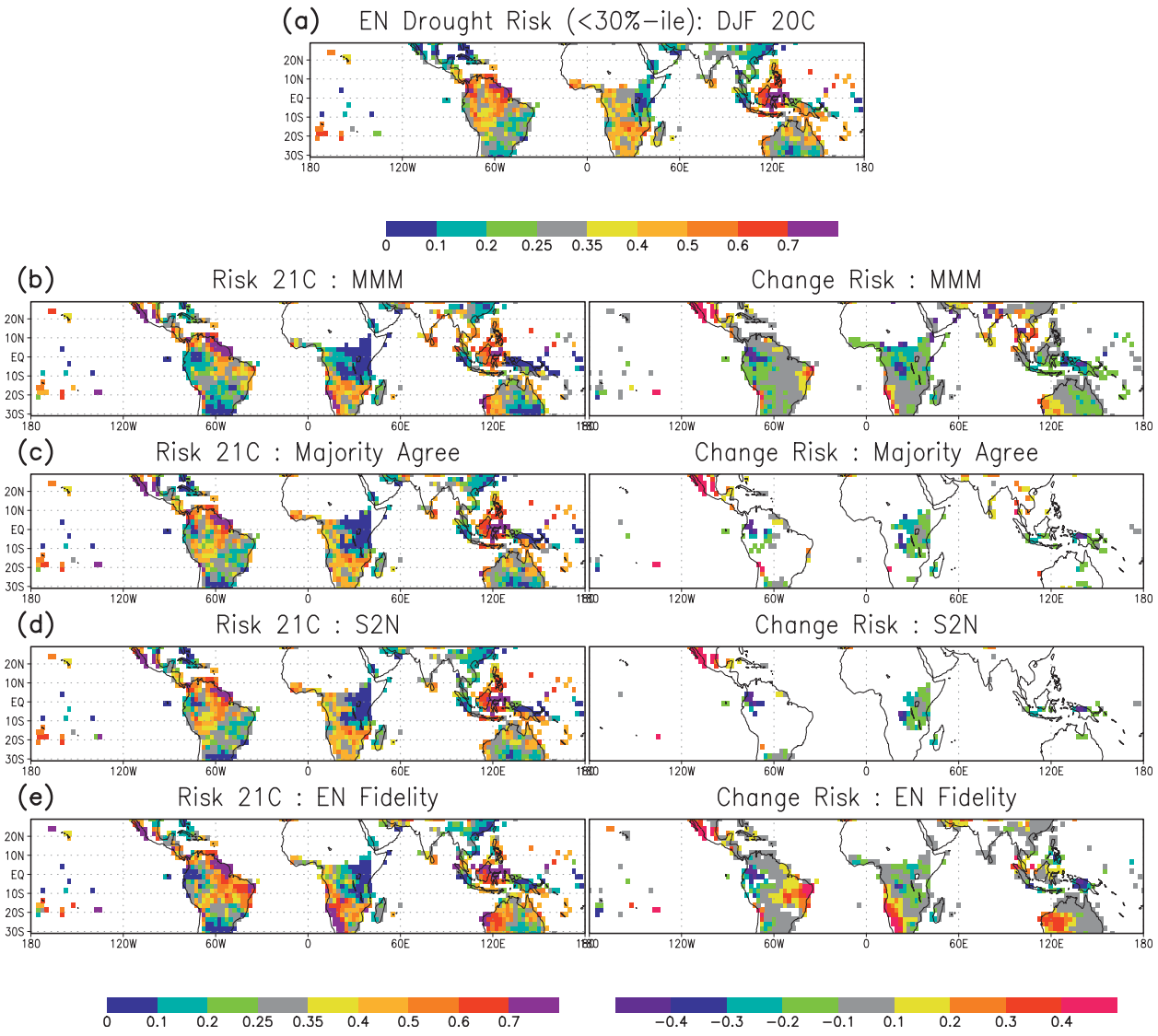

FIG. 12. Risk of deficient precipitation, defined as the 30th percentile of the observed twentieth-century distribution, during El Niño conditions for DJF (a) during the period 1959–2001; (b) during 2071–2100, based on (left) the multimodel mean (MMM) and (right) the difference [(b), left] − (a); (c) similar to (b) but only considering MMM when 7 of the 9 models agree in sign; (d) similar to (b) but only considering MMM when that value exceeds the standard deviation of the 9 models at that point; (e) similar to (b) but only considering the 4 models deemed to have realistic ENSO variability according to van Oldenborgh et al. (2005b) and additionally requiring that 3 of the 4 models agree in sign of the precipitation change. White areas in (a) and left-hand panels indicate twentieth-century mean precipitation is less than 30 mm for the season. Additional white areas in right-hand panels indicate low confidence in precipitation change or effectively no ability to predict change in El Niño–related drought risk there.

probabilities. In those cases, the drought risk probabilities remain unchanged in the left-hand panels compared to Figs. 12a and 13a, and the grid box is masked out in the maps of change in risk (e.g., Figs. 12c–e and 13c–e, right-hand side). The first case uses the multimodel mean as is (Figs. 12b and 13b), assuming all models are equally plausible, and considers the multimodel average as the best guess for the change. The second case considers model agreement (Figs. 12c and 13c), assuming that, if the majority of the models agree in their sign of the change, the multimodel mean change is more reliable. Agreement among 80% of the models (or 7 out of 9) is required, following similar analyses in the IPCC AR4. The third case more stringently requires that the multimodel mean must exceed the spread of the models (Figs. 12d and 13d) estimated by the standard deviation of the 9 model values. The final case includes only those models with realistic ENSO variability

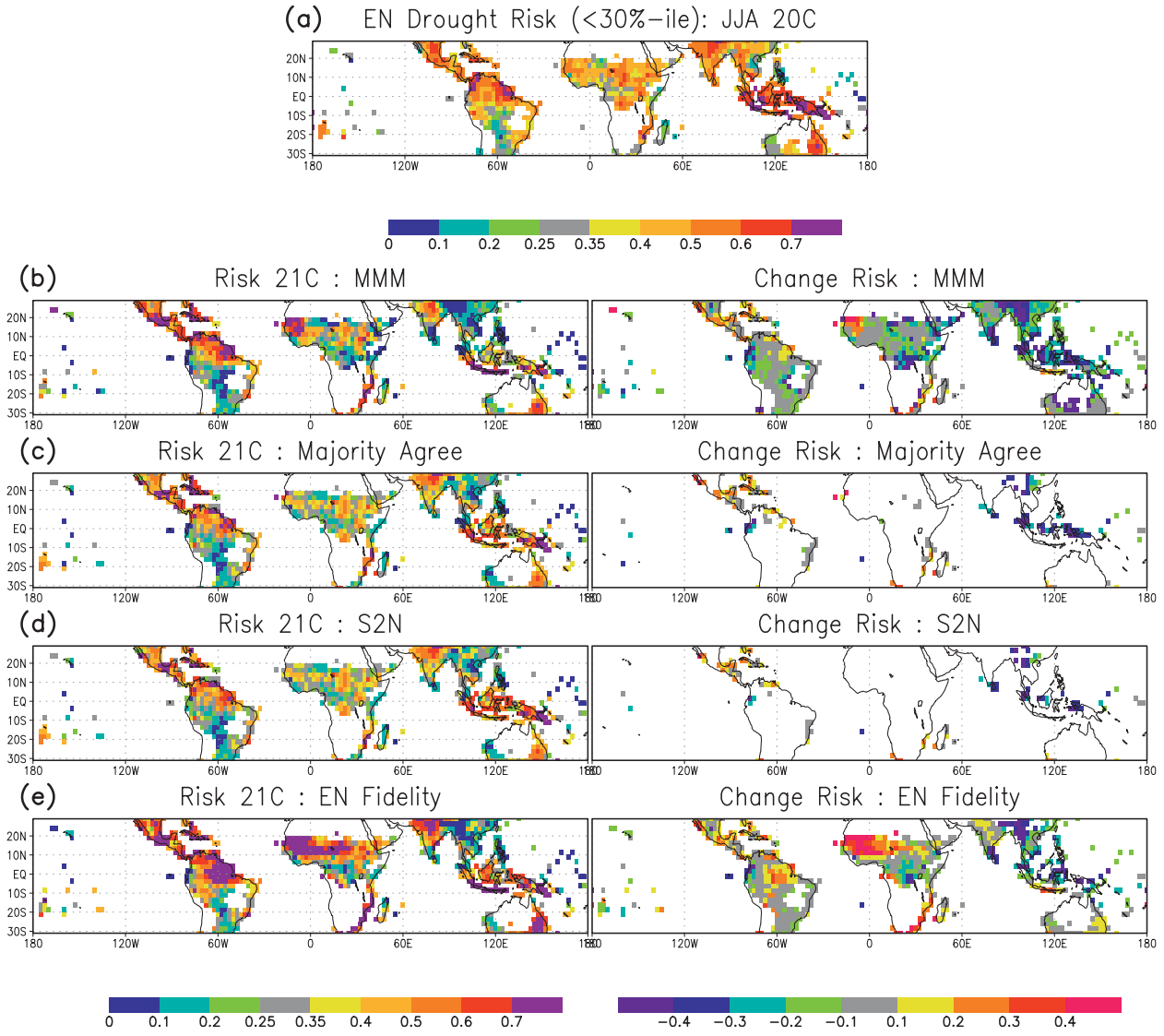

FIG. 13. As in Fig. 12, but for JJA.

(ECHAM5, GFDL 2.0, GFDL 2.1, HadCM3) according to van Oldenborgh et al. (2005b). In this final case, it is further required that at least 3 of the 4 models share the same sign of precipitation change.

The change in risk of crossing the predefined drought threshold changes similarly in the multimodel mean and the four models that reproduce realistic ENSO characteristics. However, the four models with reasonable ENSO fidelity show greater agreement among themselves and also indicate enhanced risk of drought over some of the aforementioned teleconnection regions, which seems to be only weakly shared by the other models. The significance of this finding has not been established given that this result was obtained using only 4 models. Furthermore, it has yet to be demonstrated that fidelity of climate variability in a model portends better fidelity in the forced climate change response. More important than the specific values of this analysis, however, is the example of putting the information together and the implications for confidence in the modification of climate risk depending on how one employs the climate change projection information.

6. Conclusions

This study has investigated El Niño–induced tropical droughts (in the meteorological sense, i.e., precipitation deficit) in climate change projections. Initially, diagnostics based on the projected Niño-3.4 index assessed how ENSO will behave in the twenty-first century. Next, the

spatial pattern, magnitude, range of variability, and spatial extent of El Niño–induced deficit precipitation patterns in both twentieth and twenty-first centuries was examined. Finally, a procedure for combining climate variability with change information for producing El Niño–induced drought risk estimates for the twenty-first century was illustrated. It is emphasized that the current analysis investigates only the precipitation contribution to drought, and thus the influence of increasing temperature and accompanying changes in evapotranspiration are not included. The main findings for the mature (DJF) and development (JJA) stages of El Niño can be summarized as follows:

- No significant change in relative El Niño strength or robust change in frequency is noted between climate change model simulations for the twentieth and twenty-first centuries. Based on an analysis that considers the intraensemble variability from individual models, any observed shift in ENSO characteristics will be effectively impossible to attribute to global warming.
- Climate change models that do simulate ENSO variability appropriately exhibit realistic El Niño–induced drought patterns in the twentieth century, and those are not projected to change in the twenty-first century due to global warming. To our knowledge, this is the first report on how El Niño–induced tropical drought patterns are projected to appear in the twenty-first century. Remarkably, these models produce tropical teleconnections almost as well as seasonal prediction models. Droughts observed during El Niño years in northern South America and parts of southern Africa, Indonesia, India, and Australia are consistently well reproduced by these models. The fact that both ENSO variability and the magnitude of the precipitation response remain unchanged suggests a fairly linear separation between time scales. The implications for such a separation, particularly in the context of climate risk management and climate change adaptation, are substantial.
- Furthermore, precipitation changes projected for the twenty-first century by all climate change model groups here investigated show consistency and qualitative robustness, independent of the ability of these models to simulate ENSO variability in the tropical Pacific. All three model groups project increase in tropical precipitation, particularly between 10°N and 10°S, supporting the separability between climate change and ENSO-like climate variability in the tropics.
- The spatial extent of El Niño–induced tropical droughts over land at different levels of severity is projected to be slightly reduced in the twenty-first century by all climate change models when compared to the spatial extent projected for the twentieth century. This statement is distinct from that regarding the lack of locally significant changes in El Niño precipitation impacts, in part because spatial aggregation affords a collective view of changes that are less significant at smaller spatial scales.
- The fact that El Niño–induced tropical drought patterns are not projected to change in the twenty-first century supports the use of the observed El Niño teleconnections in the twentieth century to represent future climate conditions in the twenty-first century. Because the mean climate is projected to change in the twentieth century, even if the climate variability relative to the mean climate is unchanged, the risks of a predefined event such as drought will change. A procedure for combining El Niño climate variability and projected changes in mean precipitation for the twenty-first century for estimating future drought risk for a predefined drought threshold has been illustrated. Increased risk has been found in some regions for those models that do show good fidelity in reproducing ENSO variability in the twentieth century. These changes are not an artifact of increasing or reducing ENSO variability, as it was these models that indicated no statistically robust change in El Niño characteristics. There is, however, no study to date demonstrating a coincidence between the quality of a model's representation of climate variability and change.

Acknowledgments. This research has been funded by U.S. CLIVAR Drought in Coupled Models Project (DRICOMP). CASC was supported by Fundacao de Amparo a Pesquisa do Estado de Sao Paulo (FAPESP), Processes 2005/05210-7 and 2006/02497-6. LG was supported in part under Cooperative Agreement NA05OAR4311004 between Columbia University and the National Oceanic and Atmospheric Association. We thank the EU-funded DEMETER project for making their multimodel seasonal hindcasts available at the ECMWF public data server. We also acknowledge the IPCC modeling groups, the Program for Climate Model Diagnosis and Intercomparison (PCMDI), and the WCRP's Working Group on Coupled Modeling (WGCM) for their roles in making available the WCRP CMIP3 multimodel dataset. Support of this dataset is provided by the Office of Science, U.S. Department of Energy.

REFERENCES

AchutaRao, K., and K. R. Sperber, 2006: ENSO simulation in coupled ocean-atmosphere models: Are the current models better? *Climate Dyn.,* **27,** 1–15, doi:10.1007/s00382-006-0119-7.

Barnston, A. G., M. Chelliah, and S. B. Goldenberg, 1997: Documentation of a highly ENSO-related SST region in the equatorial Pacific. *Atmos.–Ocean,* **35,** 367–383.

Clement, A. C., R. Seager, M. A. Cane, and S. E. Zebiak, 1996: An ocean dynamical thermostat. *J. Climate,* **9,** 2190–2196.

Coelho, C. A. S., D. B. Stephenson, M. Balmaseda, F. J. Doblas-Reyes, and G. J. van Oldenborgh, 2006: Towards an integrated seasonal forecasting system for South America. *J. Climate,* **19,** 3704–3721.

Collins, M., The CMIP Modelling Groups, 2005: El Niño- or La Niña-like climate change? *Climate Dyn.,* **24,** 89–104.

Dilley, M., R. S. Chen, U. Deichmann, A. L. Lerner-Lam, and M. Arnold, 2005: *Natural Disaster Hotspots: A Global Risk Analysis*. World Bank, 145 pp.

Easterling, D. R., T. W. R. Wallis, J. H. Lawrimore, and R. R. Heim Jr., 2007: Effects of temperature and precipitation trends on U.S. drought. *Geophys. Res. Lett.,* **34,** L20709, doi:10.1029/2007GL031541.

Guilyardi, E., 2006: El Niño–mean state–seasonal cycle interactions in a multi-model study. *Climate Dyn.,* **26,** 329–348.

Held, I. M., and B. J. Soden, 2006: Robust responses of the hydrological cycle to global warming. *J. Climate,* **19,** 5686–5699.

Hoerling, M., and J. Eischeid, 2007: Past peak water in the Southwest. *Southwest Hydrol.,* **6,** 18.

Knutson, T. R., S. Manabe, and D. Gu, 1997: Simulated ENSO in a global couple ocean–atmosphere model: Multidecadal amplitude modulation and CO2 sensitivity. *J. Climate,* **10,** 138–161.

Lyon, B., 2004: The strength of El Niño and the spatial extent of tropical drought. *Geophys. Res. Lett.,* **31,** L21204, doi:10.1029/2004GL020901.

Mann, H. B., and D. R. Whitney, 1947: On a test of whether one of two random variables is stochastically larger than the other. *Ann. Math. Stat.,* **18,** 50–60.

Mason, S. J., and L. Goddard, 2001: Probabilistic precipitation anomalies associated with ENSO. *Bull. Amer. Meteor. Soc.,* **82,** 619–638.

McCabe, G. J., and D. M. Wolock, 2007: Warming may create substantial water supply shortages in the Colorado River basin. *Geophys. Res. Lett.,* **34,** L22708, doi:10.1029/2007GL031764.

Meehl, G. A., and Coauthors, 2007: Global climate projections. *Climate Change 2007: The Physical Science Basis,* S. Solomon et al., Eds., Cambridge University Press, 747–846.

Merryfield, W., 2006: Changes to ENSO under CO_2 doubling in a multimodel ensemble. *J. Climate,* **19,** 4009–4027.

Misra, V., L. Marx, M. Fennessey, B. Kirtman, and J. Kinter, 2008: A comparison of climate prediction and simulation over the tropical Pacific. *J. Climate,* **21,** 3601–3611.

Mitchell, T. D., and P. D. Jones, 2005: An improved method of constructing a database of monthly climate observations and associated high-resolution grids. *Int. J. Climatol.,* **25,** 693–712.

Neelin, J. D., C. Chou, and H. Su, 2003: Tropical drought regions in global warming and El Niño teleconnections. *Geophys. Res. Lett.,* **30,** L2275, doi:10.1029/2003GL018625.

Nicholls, N., 2008: Recent trends in the seasonal and temporal behaviour or the El Niño–Southern Oscillation. *Geophys. Res. Lett.,* **35,** L19703, doi:10.1029/2008GL034499.

Nohara, D., A. Kitoh, M. Hosaka, and T. Oki, 2006: Impact of climate change on river discharge projected by multimodel ensemble. *J. Hydrometeor.,* **7,** 1076–1089.

Palmer, T. N., and Coauthors, 2004: Development of a European Multimodel Ensemble System for Seasonal-to-Interannual Prediction (DEMETER). *Bull. Amer. Meteor. Soc.,* **85,** 853–872.

Ropelewski, C. F., and M. S. Halpert, 1987: Global and regional scale precipitation patterns associated with the El Niño/Southern Oscillation. *Mon. Wea. Rev.,* **115,** 1606–1626.

Solomon, S. D. Qin, M. Manning, M. Marquis, K. Averyt, M. M. B. Tignor, H. L. Miller Jr., and Z. Chen, Eds., 2007: *Climate Change 2007: The Physical Science Basis*. Cambridge University Press, 996 pp.

Sterl, A., G. J. van Oldenborgh, W. Hazeleger, and G. Burgers, 2007: On the robustness of ENSO teleconnections. *Climate Dyn.,* **29,** 469–485.

van Oldenborgh, G. J., M. A. Balmaseda, L. Ferranti, T. N. Stockdale, and D. L. T. Anderson, 2005a: Evaluation of atmospheric fields from the ECMWF seasonal forecasts over a 15-year period. *J. Climate,* **18,** 3250–3269.

——, S. Y. Phillip, and M. Collins, 2005b: El Niño in a changing climate: A multi-model study. *Ocean Sci.,* **1,** 81–95.

Vecchi, G. A., A. Clement, and B. J. Soden, 2008: Examining the tropical Pacific's response to global warming. *Eos, Trans. Amer. Geophys. Union,* **89,** 81–83.

Wang, G., 2005: Agricultural drought in a future climate: Results from 15 global climate models participating in the IPCC 4th assessment. *Climate Dyn.,* **25,** 739–753, doi:10.1007/s00382-005-0057-9.

Wilcoxon, F., 1945: Individual comparisons by ranking methods. *Biom. Bull.,* **1,** 80–83.